

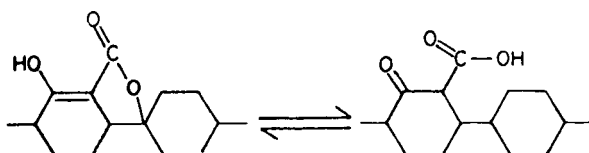
The Effect of Carbon Surface Oxides on the Enthalpy of Immersion in Water and
the Adsorption of Water Vapour

Stuart S. Barton

Department of Chemistry and Chemical Engineering
Royal Military College of Canada
Kingston, Ontario, K7K 5L0

It has been known for a long time that carbon surfaces which have been exposed to even mild oxidation, become covered to a greater or lesser extent by chemically bonded oxide groups. Depending on the temperature at which the oxidation is carried out, the carbon surface can exhibit either acidic or basic characteristics. It is likely that the surface basicity developed on high temperature oxidation is related to unsaturated "centres" produced by the thermal removal of oxides. These oxide structures are thermally unstable and may be detected by the method exemplified by Fig. 1. In this figure the differential amount of CO_2 and CO desorbed per gram of Speron 6 are shown as a function of temperature. The oxide structures which produce CO_2 are less stable than the structures which produce CO . Similar results have been obtained for other carbons.

Those oxides which are acidic can neutralize aqueous or ethanolic bases. In Fig. 2 is shown the decrease in the surface acidity of Speron 6 with increasing thermal destruction of the surface oxides. It is apparent that acidic groups of different strengths are present. However, after treatment at 800°C it appears that all acidic surface oxide has been removed. The temperature interval over which the drop in acidity occurs is the same interval over which CO_2 is desorbed. When the CO evolution has reached a maximum, however, the acidity has almost disappeared. The relationship between the basic uptake and the amount of CO_2 desorbed is shown in Fig. 3. The sodium ethoxide data fall on two intersecting straight lines. The initial line corresponds to the decomposition of the CO_2 producing oxide which is essentially complete at 600°C . This line has a slope of two indicating that the surface oxide being destroyed is dibasic. The second linear portion has a slope of one demonstrating that the less thermally stable oxide which decomposes around 250°C is monobasic. The acidic complex decomposing at 250° is not neutralized by aqueous OH^- ion whereas the 600°C desorbing species is neutralized by this base on a one to one ratio. Data of this type have been rationalized that the acid oxide group is a lactone or some similar functional group which is monobasic towards aqueous OH^- ion but can be opened into a dibasic structure by the stronger ethoxide ion. Such a structure was proposed by Garren and Weiss in 1957 i.e.



Treatment with specific chemical reagents can also provide information about the oxide structure. Diazomethane reacts quickly and smoothly with protonated sites which are carboxylate in nature to produce methyl esters. If the protonated site is phenolic then ether linkages will be formed. Since methyl esters are easily

hydrolysed while methyl ethers are resistant to hydrolysis, it is possible to discriminate between the two proton types. Fig. 4 shows data obtaining with Spheron 6. It is seen that the methoxyl content can be decreased by hydrolysis and that at least two groups are being methylated. Treatment with diazomethane for up to twenty hours produces a constant methoxyl content. After this time methylation increases slowly and becomes constant again at about 120 hours. These results are consistent with the Garten and Weiss model which implies the existence of a tautomerization step which may be very slow and rate determining.

Carbon surfaces may also be probed for protonated species by treatment with etheral Grignard reagent (methylmagnesium iodide). The gaseous hydrogen released can be measured.

All the chemical techniques outlined above were used to produce the data of Fig. 5. There is, initially, at low desorbing temperatures a considerable difference between the two methoxyl determinations (i.e. after 20 hours and 140 hours methylation) but this difference becomes smaller as degassing temperature is increased. The oxide structure which is decomposed around 250°C is apparently not methylated by diazomethane since no change in methoxyl content takes place over the range 200°-400°C. Also included in Fig. 5 are the variations of "active" hydrogen content measured by reaction with methylmagnesium iodide and the uptake of aqueous OH⁻ ion. The Grignard data fall on top of the 20 hr. reaction time results while the OH⁻ ion uptake data fall on top of the 140 hr. results. One must conclude that the slow step which retards the methylation reaction is absent during reaction with aqueous base.

A certain amount of information about the IR spectra of carbon surface oxides is also available. It has been shown in a study that a series of activated carbons, oxidized to different extents, gave IR spectra which were qualitatively similar (3 distinct bands in the 1800-1100 cm⁻¹ region). Peak areas could be quantitatively related to the amount of oxidation and, in particular, heat treatment at 1000°C produced a marked (although not complete) elimination of the spectral features.

These chemical studies and others like them, result in the conclusion that the acid surface oxides have a complex structure probably including carboxyl, phenolic and lactic features. Surface oxides which desorb as CO are also present but do not contribute to the surface acidity.

Acidic or not, all these possible structures can contribute via hydrogen bonding and other hydration interactions to the energetics of the reaction of a carbon surface with liquid and vapour water. The measurement of the enthalpy of immersion is a convenient method for the investigation of the state of a carbon surface. Either commercial calorimeters or a "home-made" instrument may be used. Fig. 6 gives a schematic diagram of a simple, easily constructed but effective calorimeter based on an original design by Zettlemoyer. The temperature sensing thermistor is part of a Wheatstone bridge. The imbalance of the bridge as a function of the heat supplied by a calibration heater gives a measure of the heat capacity of the calorimeter and its contents. Samples of carbon are outgassed carefully in thin-walled glass bulbs which are sealed under vacuum. Three or more carbon samples are immersed in water (by breaking the submerged bulb) and the slope of the heat evolved vs mass of carbon gives the enthalpy of immersion ($h_i/J \cdot g^{-1}$). This procedure automatically corrects for the "heat of breaking" i.e. the intercept on the heat axis. Typical data are shown in Fig. 7.

The change in h_i in water with outgassing temperature for graphite and Spheron 6 are given in Figs. 8,9. For both these substances h_i decreases with increasing temperature, after an initial slight increase due presumably to the removal of adsorbed water at the lower temperatures. On the other hand, h_i for

graphite in the organic liquid, benzene, stays reasonably constant as degassing temperature is increased (Fig. 10). It should be mentioned that the BET, N₂ areas of both of these adsorbents do not change appreciably with heating. Thus the h_i values obtained refers to a constant surface area. The relationship between h_i in water and the total amount of CO₂ and CO desorbed per gram (expressed as mmoles of oxygen) is shown for Spheron 6 and graphite in Figs. 11,12. The linear decrease indicates either that the energy of interaction between the two types of surface oxide (CO₂ producing and CO producing) are of the same magnitude or the CO producing site has a far stronger interaction. Probably it is the latter case which obtains.

Both graphite and Spheron 6 are not highly porous. Activated carbons, on the other hand are extremely porous. Fig. 13 shows the variation of h_i in water with outgassing temperature for the microporous carbon obtained by the vacuum pyrolysis of the polymer, polyvinylidene chloride (PVDC carbon). The surface oxide on this carbon had formed, after carbonization of the polymer, by storage in air for about six months. Fig. 14 gives the variation in h_i with total amount of oxygen thermally desorbed as CO₂ and CO. For PVDC carbon the relationship is not linear and a very large drop in h_i value takes place when the initial amounts of oxide are removed. It is obvious that unlike the case with the non-porous carbons, there is a source of interaction with water other than the surface oxides. This source must involve the pore structure. It is interesting to compare the rates of decrease of h_i with surface oxide removal, given in Table I. The second column of this table is simply the slope of the linear portions of the h_i vs oxygen removed curves of Figs. 11 and 12. For PVDC carbon linearity is not strictly followed and then only after most of the oxide has been removed.

TABLE I

	Slope J-mol ⁻¹	h _i J-g ⁻¹	Oxide mmol-g ⁻¹	h _o J-g ⁻¹	h _o J-g ⁻¹	BET m ² -g ⁻¹
Graphite	-10	13.0	0.569	5.7	7.3	160
Spheron 6	-9.2	11.6	0.703	6.5	5.1	120
PVDC carbon	----	50.2	1.45	21.7	28.5	---

For graphite and Spheron 6, where linearity is found, the slope gives the water-oxide interaction energy per mole of oxide site. For graphite and Spheron 6, the product of the slope and the oxygen desorbed at 1000°C gives the contribution to the overall h_i from oxide water interactions (h_o). These quantities when subtracted from the initial h_i values give the contribution from the "bare" carbon surface (h_c). Naturally, these latter are very close to the h_i of the 1000°C degassed samples and are proportional to the BET surface areas of the non-porous carbons. This simple analysis cannot be applied to the porous carbon where there appears to be some synergistic effect involving pore and oxide sites which contributes disproportionately to h_i. This behaviour may be explored by a different method in which h_i is measured for a series of PVDC carbon samples pre-covered with known amounts of water. The results of such a study are shown in Fig. 15. The slope of the curve is the net molar enthalpy of adsorption ($\Delta\bar{H}$). The data indicate that there are two distinct $\Delta\bar{H}$ values. Up to about 0.6 mmol-g⁻¹ adsorption $\Delta\bar{H}$ is 24 kJ-mol⁻¹. Further adsorption proceeds with $\Delta\bar{H} = 1.7 \text{ kJ}\cdot\text{mol}^{-1}$. At the point of the change from the high $\Delta\bar{H}$ to the low $\Delta\bar{H}$, the h_i value is 28.5 J-g⁻¹. This figure is very close to the h_i obtained with PVDC carbon degassed at 1000°C. This value then, represents the contribution from pore

filling and when it is subtracted from the initial h_i produces the contribution for water-oxide interactions (21.7 J-g^{-1}). A value for the energy of interaction of water per mole of oxide site for PVDC carbon may now be computed as $21.7/1.45 = 15 \text{ J-mole}^{-1}$. This larger value must reflect the synergetic effect referred to earlier.

The preceding analysis purports to show that it is possible to obtain from appropriate experiments the contribution to the overall interaction from oxide sites, bare open carbon surface and pore filling. Obviously much more work must be done before the validity of such an analysis can be established.

The dramatic changes in water vapour adsorption which can result from the presence of surface oxides is illustrated in Fig. 16. The figure shows the isotherms obtained after evacuation at 40°C of carbon cloth which had been progressively oxidized in 6M HNO_3 . The "as received" material produces a typical sigmoid (Type V) isotherm. The oxidized samples, on the other hand, show Type I or Langmuir behaviour. Values of h_i and ΔH also increase greatly on oxidation. After evacuation at 400°C , when much of the oxide has been destroyed, the water vapour isotherms are all Type V.

If time permits application of immersional enthalpy measurement to complex solids such as coal will be examined.

BIBLIOGRAPHY

This discussion is based on the following articles:

- S.S. Barton and B.H. Harrison, CARBON 10, 245 (1972).
- S.S. Barton, B.H. Harrison and G.L. Boulton, CARBON 10, 395 (1972).
- S.S. Barton, B.H. Harrison and D. Gillespie, NATURE 235, 134 (1971).
- S.S. Barton and B.H. Harrison, CARBON 13, 47 (1975).
- S.S. Barton, B.H. Harrison and D. Gillespie, CARBON 16, 363 (1978).
- S.S. Barton, M.J.B. Evans and B.H. Harrison, J. COLL. INTERFACE SCI. 45, 542 (1973).
- S.S. Barton and J.E. Koresh, J. CHEM. SOC. FAR. TRANS. I 79, 1173 (1983).
- S.S. Barton, J.R. Dacey and M.J.B. Evans, COLL&POLYMER SCI. 260, 726 (1982).

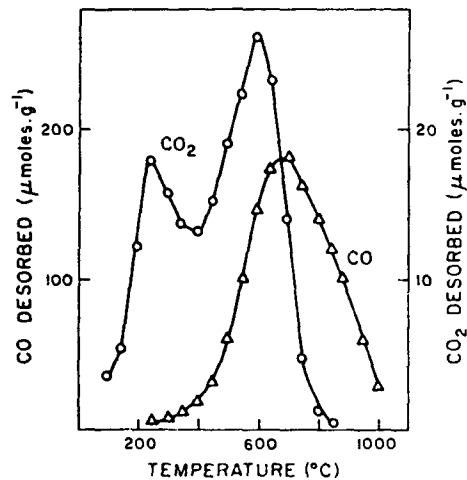


Fig. 1 Differential gas evolution curve.

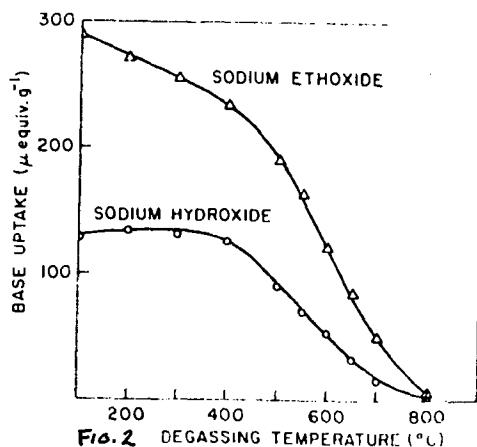


Fig. 2 DEGASSING TEMPERATURE (°C)

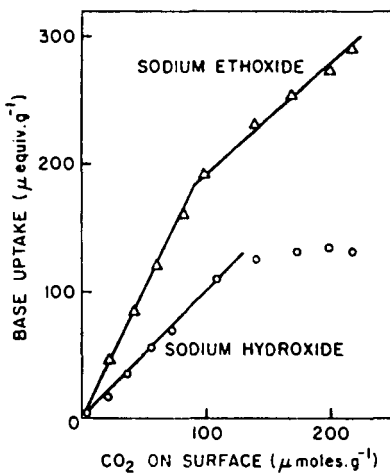


Fig. 3 Relation between base uptake and the oxides desorbing as CO_2 .

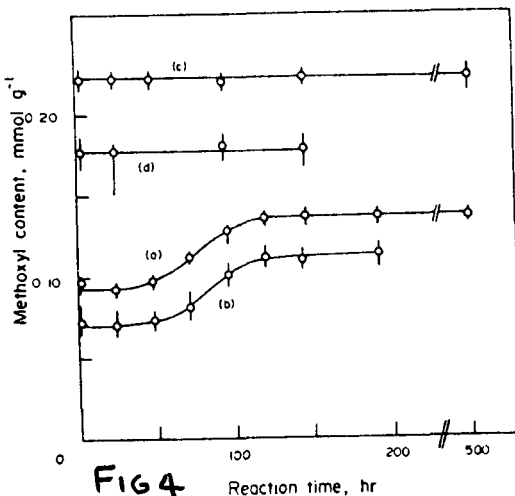


FIG 4

Reaction time, hr

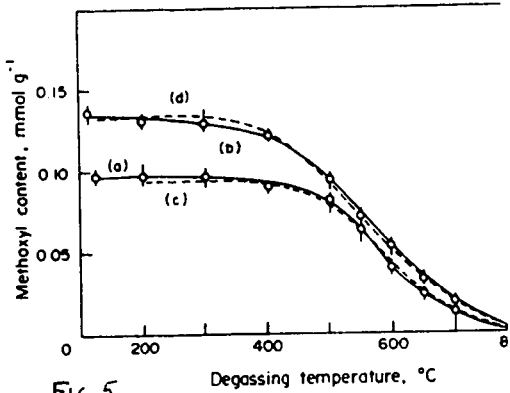


Fig. 5

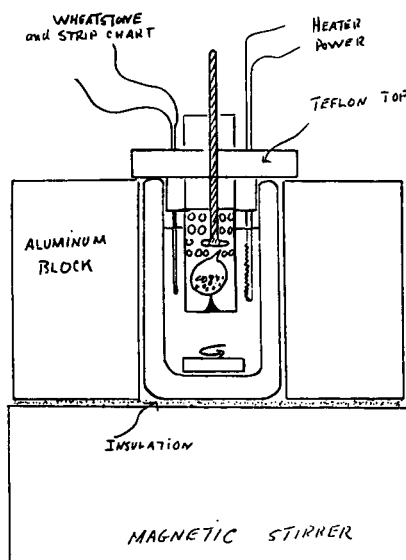


Fig. 6

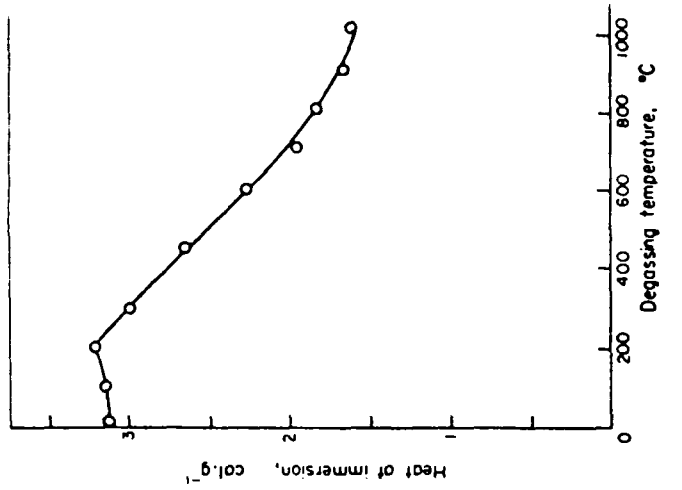


Fig. 8 Heat of immersion of graphite, degas. temperatures up to 1000°C, in water.

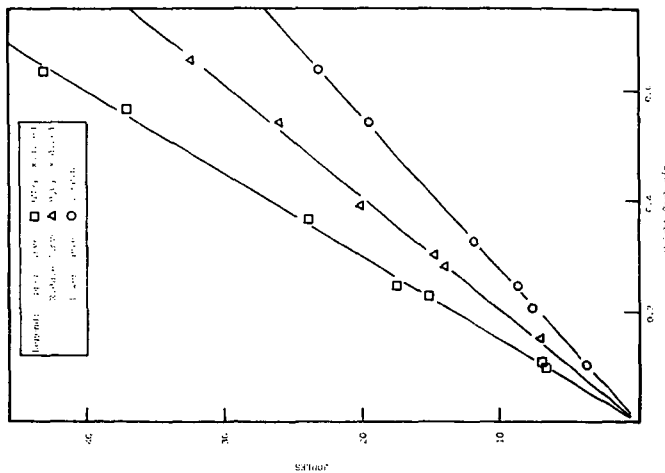


Fig. 9 Heat of immersion in water

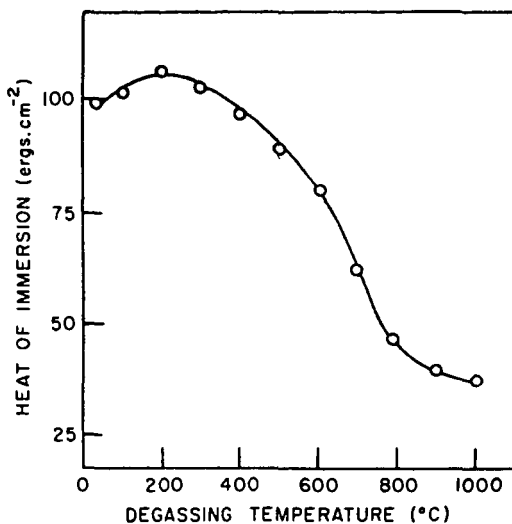


Fig. 9 Heat of immersion of Spheron 6, degassed at various temperatures, in water.

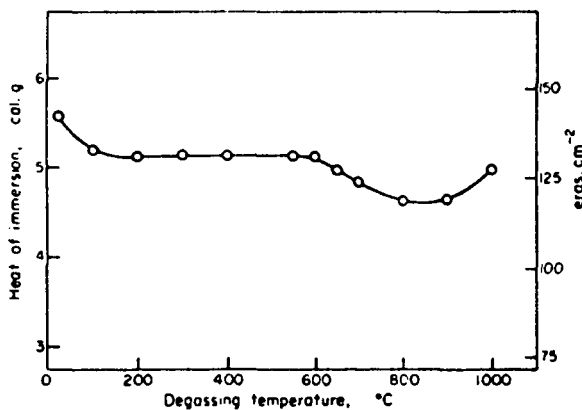


Fig. 10 Heat of immersion of graphite, degassed at temperatures up to 1000°C, in benzene.

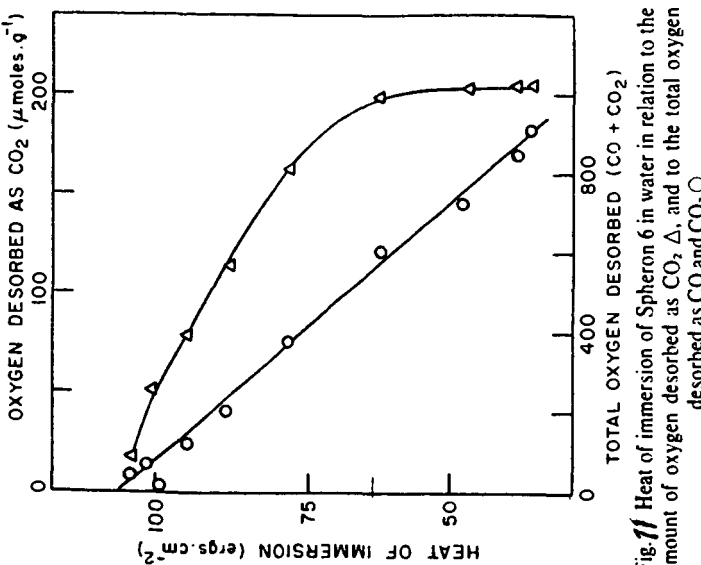


Fig. 11 Heat of immersion of Spheron 6 in water in relation to the amount of oxygen desorbed as CO₂, Δ, and to the total oxygen desorbed as CO and CO₂, ○.

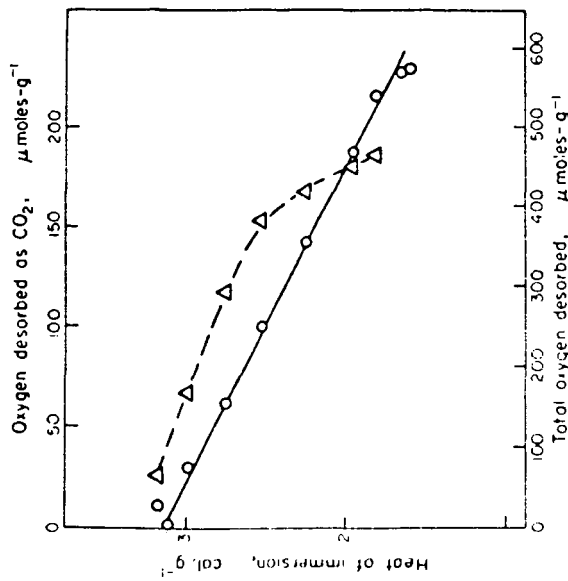


Fig. 12 Heat of immersion of graphite in water in relation to the amount of oxygen desorbed as CO₂, Δ, and to the total oxygen desorbed as CO and CO₂, ○.

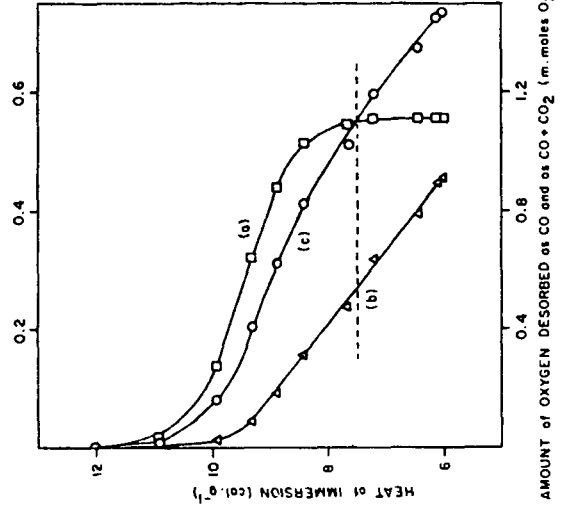


Fig. 14 Heat of immersion of PVDC carbon plotted as a function of (a) oxygen desorbed as CO_2 , (b) oxygen desorbed as CO , (c) total oxygen ($\text{CO} + \text{CO}_2$).

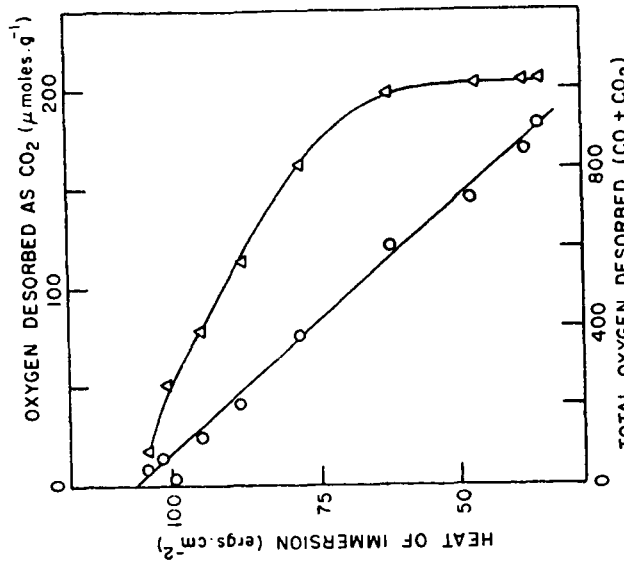


Fig. 15 Heat of immersion of Spheron 6 in water in relation to the amount of oxygen desorbed as CO_2 , Δ , and to the total oxygen desorbed as CO and CO_2 .

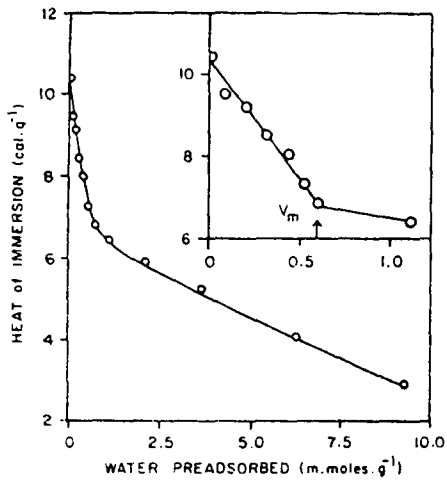


FIG. 15—Effect of ppreadsorbing water on the heat of immersion in water.

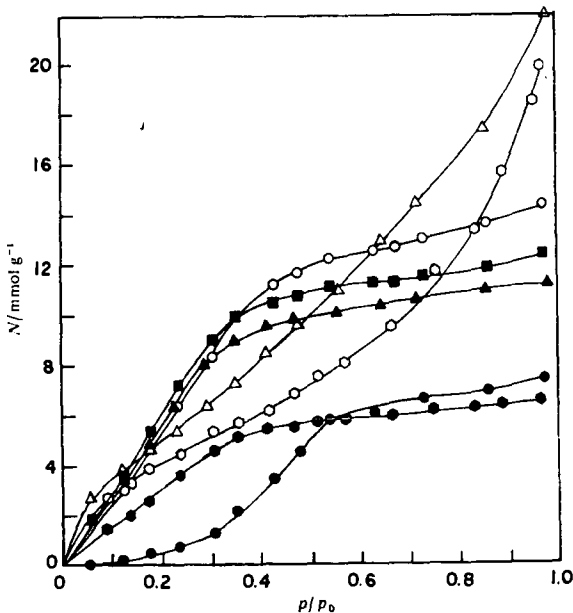


FIG. 16—Absolute water isotherms at 25 °C on the following air-activated carbons: ●, as received; ●, Ox-HNO₃-2; ▲, Ox-HNO₃-3; ■, Ox-HNO₃-4; ○, Ox-HNO₃-6; Δ, Ox-HNO₃-12; ○, Ox-HNO₃-16.